

Growth Kinetics and Modeling of ZnO Nanoparticles

Penny S. Hale,^{*†} Leone M. Maddox, Joe G. Shapter, and Nico H. Voelcker

School of Chemistry, Physics and Earth Sciences (SoCPES), Flinders University of South Australia, GPO Box 2100, Adelaide, 5000, Australia; *p.hale@latrobe.edu.au

Michael J. Ford

Institute of Nanoscale Technology, University of Technology, Sydney, PO Box 123, Broadway, NSW, 2007, Australia

Eric R. Waclawik

School of Physical and Chemical Sciences, Queensland University of Technology, 2 George Street, GPO Box 2434 Brisbane, QLD, 4001, Australia

Nanotechnology is a new and exciting area of research that is investigating, among other things, the use of nano-sized particles in technological applications. Zinc oxide particles less than 100 nm in diameter, for example, are optically clear (transparent in visible light) but opaque to UV light and are being touted as the sunscreen of the future (1). The nanoparticles provide an excellent barrier to UV light, are non-allergenic, and can be incorporated into many cosmetics. Zinc oxide is also a semiconductor and fluoresces in both the UV and visible regions. The peak in fluorescence shifts as a function of particle size (2). These properties make ZnO nanoparticles an interesting system to study with many different applications.

Unfortunately, students are rarely introduced to current topics of scientific interest. Flinders University started one of the first undergraduate degrees specializing in nanotechnology (3). Part of the program involves using examples of new technology and new materials applications in the laboratory course to spark the interest of students who are already focused on these current topics in their lectures. Several experiments from this *Journal* have been used for this purpose (4, 5). This laboratory aims to highlight key features of nanoparticulate systems and introduces a model that students can manipulate to try to understand the different parameters affecting absorption properties. The laboratory can also be used in undergraduate inorganic or physical chemistry courses to introduce colloid chemistry and growth kinetics and would stimulate discussion in a number of related areas. Our nanotechnology students have a strong physics background, so concepts such as band-gap energy and effective mass are covered in courses on solid-state physics. When adapting this laboratory for chemistry students an appropriate discussion on these concepts should be included (6).

This experiment is based upon an article by Wong et al. (7) that used the spectroscopic properties of quantum-sized zinc oxide to study growth kinetics using a method initially developed by Bahnemann et al. (2). The technique for producing quantum-sized ZnO particles is much safer than a technique previously published in this *Journal* (8) that used hydrogen sulfide gas to produce cadmium sulfide and zinc sulfide nanoparticles. A further advantage of this method is

the ability to sample the solution over time and hence determine the growth kinetics. The procedure was incorporated into the third-year laboratory program for nanotechnology and introduced particularly relevant concepts such as growth kinetics and measurement of the size of nanoparticles. Students measured the absorbance of ZnO colloids over time and determined the band gap energy. From this data they calculated the diffusion coefficient of the particles in ethanol using both the Ostwald model and Stokes–Einstein equation. The laboratory was extended by applying a general model for absorption by small particles (9).

Theory

In a semiconductor such as ZnO, light is only absorbed if it has a frequency (and hence energy) that is greater than the energy required to excite an electron from the valence band to the conduction band of the material. This promotion of the electron to the conduction band creates a positively-charged hole in the valence band. There is a strong attraction between the negatively-charged electron and the positively-charged hole, causing them to orbit each other. They form a stable species called an exciton. In bulk semiconductors, the electron and hole orbit each other at a distance that depends on the semiconductor's dielectric constant. When semiconductor particles are synthesized with dimensions smaller than the natural exciton radius (called the Bohr radius) quantum-size effects occur. For instance, ZnO nanoparticles smaller than 20 nm absorb light at a shorter wavelength than bulk particles. This is because energy is now required to confine the exciton within the nanoparticle. In fact only particular (discrete) exciton energies are allowed. Exciton confinement induces quantization of energy. For this reason semiconductor nanoparticles are also called quantum dots.

The position of the exciton transition of a colloidal system depends on the particle size and shape, solvent or adsorbate refractive index, and the interparticle distance. For ZnO particles about 3 nm in diameter, the absorbance maximum (λ_{max}) is around 365 nm. For smaller colloids, a slight (few nanometer) blue shift is expected, whereas for larger colloids, red-shifting of this band is observed. The peak width gives information about the polydispersity of the colloidal solution, with broader peaks indicating a greater distribution in particle size.

[†]Current address: Centre for Materials and Surface Science, Department of Physics, Faculty of Science, Technology and Engineering, La Trobe University, Victoria 3086, Australia.

Particle-Size Determination

The particle size can be determined experimentally from the absorption spectra using the effective-mass model (10)

$$E_g^* \cong E_g^{\text{bulk}} + \frac{\hbar^2 \pi^2}{2r^2} \left(\frac{1}{m_e^* m_e} + \frac{1}{m_h^* m_e} \right) - \frac{1.8e^2}{4\pi\epsilon\epsilon_0 r} - \frac{0.124e^4}{\hbar^2 (4\pi\epsilon\epsilon_0)^2} \left(\frac{1}{m_e^* m_e} + \frac{1}{m_h^* m_e} \right)^{-1} \quad (1)$$

where E_g^* is the band gap energy for the particle, E_g^{bulk} is the bulk band gap energy (for ZnO, $E_g^{\text{bulk}} = 3.4$ eV), \hbar is Planck's constant ($\hbar/2\pi$), r is the particle radius, m_e^* is the effective mass of electrons, m_h^* is the effective mass of holes, m_e is the free electron mass, e is the charge on an electron, ϵ_0 is the permittivity of free space, and ϵ is the relative permittivity of the solid. The particle size can be obtained from the band gap energy inferred from the optical absorption spectra. The band gap energy, E_g^* , can be determined from the cut-off wavelength ($E_g^* = hc/\lambda_c$). The particle size (sphere with a radius of about 3 nm) obtained from this method is slightly larger than that determined by other techniques such as transmission electron microscopy (TEM) or X-ray diffraction (XRD) (about 2 nm). This is possibly because the cut-off wavelength is related more to the size distribution of particles and hence the estimated size appears slightly larger than the average particle size. A tight-binding model can also be used and has been shown to give closer agreement to experimental data (10) but requires understanding of quantum systems at a higher level than most chemistry students attain.

Growth Kinetics

Initially, a solution will contain a large number of small particles or crystals. Because of surface tension (and surface-to-volume ratios), small particles are much more soluble than large particles. The small particles will be precipitated onto larger particles. The small particles therefore act as "nutrients" for bigger particles and the average particle size will increase. The rate of this process, called Ostwald ripening, decreases as the particles grow and the particle size distribution becomes narrower.

This spontaneous process occurs because larger particles are more energetically favored than smaller particles. While the formation of many small particles is *kinetically* favored, (i.e., they nucleate more easily) large particles are *thermodynamically* favored. This is because small particles have a larger surface area-to-volume ratio than large particles and are consequently easier to produce. Molecules on the surface are energetically less stable than the ones already well ordered and packed in the interior. Large particles, with their greater volume-to-surface area ratio, therefore represent a lower-energy state. Hence, many small particles will attain a lower-energy state if transformed into large particles and this is what we see in Ostwald ripening.

The rate law can be derived (7) from the Gibbs–Thomson equation and Fick's law, but the main result is:

$$\bar{r}^3 = Kt; \quad \text{where } K = \frac{8\gamma DV_m^2 C_\infty}{9RT} \quad (2)$$

and \bar{r} is the average particle radius, C_∞ is the equilibrium

concentration at a flat surface, γ is the interfacial energy, V_m is the molar volume of the solid (mol cm^{-3}), D is the diffusion coefficient, R is the gas constant, and T is the temperature (K). Hence a plot of particle size cubed versus time should be linear if the particle growth follows Ostwald ripening. The diffusion coefficient from the Stokes–Einstein equation for ionic diffusion can be compared to the Ostwald model by comparing the diffusion coefficient obtained from the graph to that obtained from

$$D = \frac{k_B T}{6\pi\eta a} \quad (3)$$

where a is the hydrodynamic radius of the solute, η is the viscosity of the solvent, and k_B is Boltzmann's constant.

It should be noted that if access to a particle size analyzer is possible, complementary results can be obtained. Since many of these instruments measure the diffusion of particles and estimate the hydrodynamic radius from the Stokes–Einstein equation, the results would illustrate the differences between the models used in each case.

Modeling

The absorbance, A , of a dilute solution of small particles can be calculated from Mie theory (11)

$$A = \frac{CNl}{2.303} \quad (4)$$

where C is the absorption cross section, N is the number of particles per unit volume and l is the optical path length (cm). The absorption cross section is dependent on the dielectric properties of the particle and the surrounding medium and in the limit where the circumference of the particle is less than the wavelength of light the cross section can be expressed as (9)

$$C = \frac{24\pi^2 r^3 \epsilon_m^{3/2}}{\lambda} \frac{\epsilon''}{(\epsilon' + 2\epsilon_m)^2 + \epsilon''^2} \quad (5)$$

where r is the radius of the particle and ϵ_m is the dielectric permittivity for the medium (constant). The dielectric permittivity for the particle (ϵ) may be affected by a number of factors; size quantization (in semiconductors), conduction electron scattering (in metal particles as the particles become smaller) or physicochemical effects. The dielectric permittivity of the particle contains real and imaginary parts:

$$\epsilon = \epsilon' + i\epsilon'' \quad (6)$$

The origin of a strong absorption peak in metallic colloids can be clearly seen from eq 5, when $\epsilon' = -2\epsilon_m$ (if ϵ'' small). This generally occurs when $\epsilon' < 0$ in the UV–visible part of the spectrum (12). Hence, the peak can shift with particle size and color changes may be observed if the peak absorbance is in the visible region (as with gold colloids).

The dielectric response of a metal can be described by the simple Drude model where the dielectric permittivity is dependent upon the frequency of the incident light, a damping constant, and a plasma frequency, which is dependent on the material properties. At particle sizes smaller than the mean free path of an electron, the conduction electrons are scattered by the surface of the sphere and the damping constant becomes size dependent.

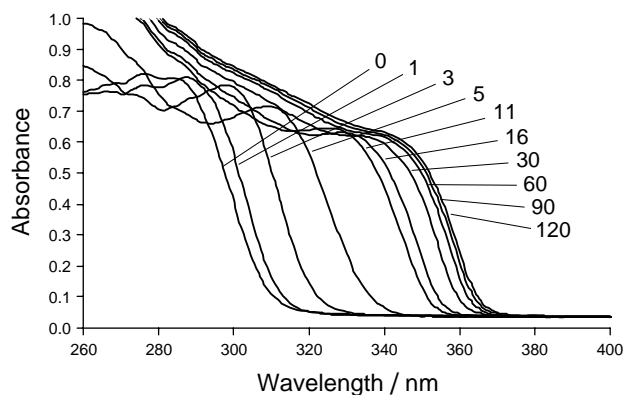


Figure 1. Absorption spectra for a colloid aged at 65 °C. The spectra were recorded at 0, 1, 3, 5, 11, 16, 30, 60, 90, and 120 min after immersion in the aging water bath.

For semiconductor particles no such theory exists. Strong changes in ϵ' occur near the band edge of semiconductors, but normally negative values are not encountered. As such, the absorption spectrum of small, non-quantized semiconductor particles resembles that of the bulk material (12).

The dielectric data for ZnO are only available for particles greater than 6 nm (13). However, the absorption can be calculated from the bulk dielectric data and compared to the experimental spectrum and the effect of the dielectric medium can be investigated.

Experimental

The students prepared solutions of 1 mM zinc acetate and 0.02 M sodium hydroxide in isopropanol and chilled both solutions to 0 °C. The solutions were then combined at 0 °C while stirring and then placed in a water bath at 65 °C. The temperature of the water bath could be between 35 and 75 °C but to be able to see a significant change in two hours of sampling, temperatures greater than 50 °C are suggested.

The solution was sampled regularly and the absorption spectrum was measured in a UV-vis spectrophotometer (Cary 50). Since the growth rate slowed over time, more samples were analyzed initially. The suggested times were 0, 1, 3, 5, 10, 15, 30, 60, 90, and 120 minutes. A typical set of results obtained by students is shown in Figure 1.

Hazards

Using isopropanol at this temperature can cause harmful vapors so the procedure should be carried out in a well-ventilated room and safety glasses worn at all times. Care must be taken when handling hot liquids.

Results

The initial preparation of the colloid was allocated a three-hour laboratory period. The modeling section was completed the following week in the next laboratory session but could be assigned as homework. The particle size was deter-

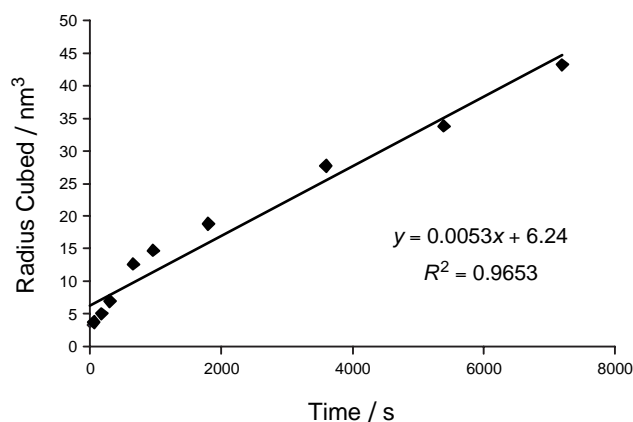


Figure 2. Cube of the particle radius versus aging time at 65 °C.

mined from the spectra (shown in Figure 1) and plotted against time as shown in Figure 2 to determine the kinetics of growth. The diffusion coefficient was estimated for Ostwald ripening from the graph (from Figure 2, $D = 1.96 \times 10^{-9} \text{ m}^2 \text{ s}^{-1}$) and compared to that for Stokes-Einstein diffusion for isopropanol at the appropriate temperature ($D = 1.04 \times 10^{-9} \text{ m}^2 \text{ s}^{-1}$ at 65 °C). The Stokes-Einstein diffusion coefficient was calculated using a hydrodynamic radius of 0.51 nm and a viscosity of 0.465 mPa, which was extrapolated to 65 °C from the *CRC Handbook* (14) values at lower temperatures. The diffusion coefficients show there was good agreement between the models. Typically, students obtained diffusion coefficients within the same order of magnitude.

The main problem students had was in estimating the cut-off wavelength from the absorption spectra. Nedeljkovic et al. (8), introduced a method where the slope of the peak was estimated and the cut-off wavelength measured from where the tangent crossed the λ axis. This method, while not perfect, was simple for students to use and gave reasonable results. An alternative method whereby the tangent was determined at half the peak maximum was trialled but the results were, on average, too small. This method for determining particle size can be used as an additional analytical technique when working with colloids or nanoparticles and can be used in combination with XRD or particle size analyzers. In fact, later versions of this practical used a particle size analyzer¹ as well as a UV-vis spectrometer so that comparisons could be made.

If no modeling was required the laboratory could be left at that point, with a brief understanding of colloids and their growth. This would be suitable for most chemistry students and would only require one laboratory session (three hours). Since the nanotechnology students have a strong physics background a more comprehensive investigation of colloid properties was completed in the modeling section. To allow chemistry students to complete this section a more appropriate introduction to semiconductors similar to Kippeny et al. (6) should be included.

Students were required to look up tables of constants for the different parameters (15, 16) and use them in their respective equations to calculate absorbance. A table of the zinc oxide dielectric data was supplied and is included in the

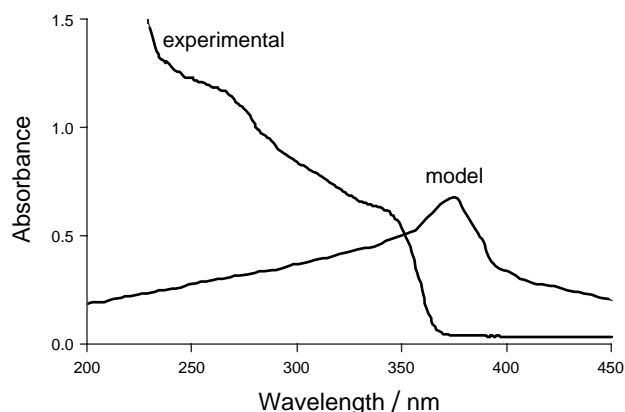


Figure 3 Absorption spectra from a model for 6-nm zinc oxide particles in isopropanol compared with experimental spectra of 3-nm particles in isopropanol.

Supplemental Material.^W The constants used in calculations are also supplied. The key parameters that students were asked to investigate were the particle size and the effect of the solvent. The resulting theoretical curves were compared to experimental curves (Figure 3) and students were asked to explain the reasons for differences. The main differences are in the position and width of the peak and the background shape. Since the model is based on 6-nm particles, the peak is expected to be redshifted with respect to the experimental curve. The second peak about 270 nm can be attributed to smaller particles in the solution. The distribution of particle sizes will contribute to the peak width and solvent effects are most likely to produce the large background. Filtering the solutions with microporous filters may reduce this background.

The choice of program to set up and manipulate these equations was left to the student. It has been achieved in Microsoft Excel as is shown in Figure 3, but students have also used more mathematical programs such as Maple. Simple software could also be written so students could simply enter the parameters to get the final absorption spectra but this was outside the scope of the experiment and was not tried.

Conclusions

There are a number of ways to extend this experiment. The theory given is for upper-level undergraduate students but could be extended to include the whole Lifshitz–Slyozov–Wagner (LSW) method of modeling particle growth. The assumptions of this model do not always hold for colloidal suspensions and several corrections can be made (2). Other models, such as the tight-binding model could also be explored. These are certainly issues that can be discussed during a complementary lecture course. Other extensions could include investigating the mechanism of formation of nanoparticles from the chemical perspective (17) or completing the experiment at different temperatures.

The student response to this experiment was encouraging. Their ability to link theory and experiment was developed using the modeling section and students became more aware of the parameters affecting absorption in nanoparticle suspensions. The use of concepts and constants from solid-state theory al-

lowed students to make links between the physics and the chemistry and realize the value of each approach. These outcomes were realized from the students' answers to the questions at the end of the laboratory (as presented in the Supplemental Material^W) and from their questions to demonstrators.

An ideal extension of this laboratory would be to investigate more thoroughly the dielectric model for metallic colloids and to use this model to identify the size of a gold or silver colloid (9). An attempt to use the model for zinc metal particles was not successful, as some critical parameters are not well known. Gold and silver are some of the more widely studied colloids and hence accurate data are widely available (5).

^WSupplemental Material

Instructions for the students, including lab questions, experimental constants, and dielectric data, and notes for the instructor are available in this issue of *JCE Online*.

Acknowledgment

We thank Paul Mulvaney from Melbourne University for the useful discussions and advice when investigating the modeling of adsorption spectra.

Note

1. High Performance Particle Sizer from Malvern Instruments, United Kingdom (Model Number HPP5001).

Literature Cited

1. Innes, B. T. T.; Dawkins, H.; Dunlop, J.; Trotter, G.; Nearn, M.; McCormick, P. G. Presented at the Aust Society for Cosmetic Chemists Conference, 2002 (unpublished). Available from <http://www.apr-powders.com/zinclear.php> (accessed Feb 2005).
2. Bahnemann, D. W.; Kormann, C.; Hoffmann, M. R. *J. Phys. Chem.* **1987**, *91*, 3789.
3. Shapter, J. G.; Ford, M. J.; Maddox, L. M.; Wacławik, E. R. *Int. J. Eng. Ed.* **2002**, *18*, 512.
4. Berger, P.; Adelman, N. B.; Beckman, K. J.; Campbell, D. J.; Ellis, A. B.; Lisensky, G. C. *J. Chem. Educ.* **1999**, *76*, 943.
5. Keating, C. D.; Musick, M. D.; Keefe, M. H.; Natan, M. J. *J. Chem. Educ.* **1999**, *76*, 949.
6. Kippeny, T.; Swafford, L. A.; Rosenthal, S. J. *J. Chem. Educ.* **2002**, *79*, 1094.
7. Wong, E. M.; Bonevich, J. E.; Searson, P. C. *J. Phys. Chem. B* **1998**, *102*, 7770.
8. Nedeljkovic, J. M.; Patel, R.; Kaufman, P.; Joyce-Pruden, C.; O'Leary, N. *J. Chem. Educ.* **1993**, *70*, 342.
9. Mulvaney, P. *Langmuir* **1996**, *12*, 788.
10. Brus, L. E. *Nanostructured Materials* **1992**, *1*, 71.
11. Bohren, C. F.; Huffman, D. R. *Absorption and Scattering of Light by Small Particles*; Wiley: New York, 1983.
12. Mulvaney, P. *Stud. Surf. Sci. Cat.* **1997**, *103*, 99.
13. Kolb, D. M.; Schulz, H. J. *Curr. Top. Mater. Sci.* **1981**, *7*, 226–268.
14. *CRC Handbook of Chemistry and Physics*, 53rd ed.; CRC Press: Boca Raton, FL, 1972.
15. Kittel, C. *Introduction to Solid State Physics*, 7th ed.; John Wiley and Sons Inc.: New York, 1996.
16. Ashcroft, N. W.; Mermin, N. D. *Solid State Physics*; Rinehart and Winston: New York, 1976.
17. Imbushii, Y.; Takami, R.; Iwasaki, M.; Ito, S. *J. Colloid Interface Sci.* **1998**, *200*, 220.